EUROPEAN LABORATORY FOR PARTICLE PHYSICS (CERN)

Search for sleptons in e^+e^- collisions at centre–of–mass energies of 161 GeV and 172 GeV

The ALEPH Collaboration

Abstract

The data recorded by the ALEPH experiment at LEP at centre–of–mass energies of 161 GeV and 172 GeV were analysed to search for sleptons, the supersymmetric partners of leptons. No evidence for the production of these particles was found. The number of candidates observed is consistent with the background expected from four–fermion processes and $\gamma\gamma$–interactions. Improved mass limits at 95% C.L. are reported.

Submitted to the 1997 lepton-photon conference, Hamburg

The ALEPH Collaboration

R. Barate, D. Buskulic, D. Decamp, P. Ghez, C. Goy, J.-P. Lees, A. Lucotte, M.-N. Minard, J.-Y. Nief, B. Pietrzyk

Laboratoire de Physique des Particules (LAPP), IN^{2}P^3-CNRS, 74019 Annecy-le-Vieux Cedex, France

M.P. Casado, M. Chmeissani, P. Comas, J.M. Crespo, M. Delfino, E. Fernandez, M. Fernandez-Bosman, Ll. Garrido,[15] A. Juste, M. Martinez, R. Miquel, Ll.M. Mir, S. Orteu, C. Padilla, I.C. Park, A. Pascual, J.A. Perlas, I. Riu, F. Sanchez, F. Teubert

Institut de Física d'Altes Energies, Universitat Autònoma de Barcelona, 08193 Bellaterra (Barcelona), Spain[7]

A. Colaleo, D. Creanza, M. de Palma, G. Gelao, G. Iaselli, G. Maggi, M. Maggi, N. Marinelli, S. Nuzzo, A. Ranieri, G. Raso, F. Ruggieri, G. Selvaggi, L. Silvestris, P. Tempesta, A. Tricomi,[3] G. Zito

Dipartimento di Fisica, INFN Sezione di Bari, 70126 Bari, Italy

X. Huang, J. Lin, Q. Ouyang, T. Wang, Y. Xie, R. Xu, S. Xue, J. Zhang, L. Zhang, W. Zhao

Institute of High-Energy Physics, Academia Sinica, Beijing, The People's Republic of China[8]

D. Abbaneo, R. Alemany, A.O. Bazarko,[1] U. Becker, P. Bright-Thomas, M. Cattaneo, F. Cerutti, G. Dissertori, H. Drevermann, R.W. Forty, M. Frank, R. Hagelberg, J.B. Hansen, J. Harvey, P. Janot, B. Jost, E. Kneringer, J. Knobloch, I. Lehraus, G. Lutters, P. Mato, A. Minten, L. Moneta, A. Pacheco, J.-F. Pusztaszeri,[20] F. Ranjard, G. Rizzo, L. Rolandi, D. Rousseau, D. Schlatter, M. Schmitt, O. Schneider, W. Tejessy, I.R. Tomalin, H. Wachsmuth, A. Wagner[21]

European Laboratory for Particle Physics (CERN), 1211 Geneva 23, Switzerland

Z. Ajaltouni, A. Barrès, C. Boyer, A. Falvard, C. Ferdi, P. Gay, C . Guicheney, P. Henrard, J. Jousset, B. Michel, S. Monteil, J-C. Montret, D. Pallin, P. Perret, F. Podlyski, J. Proriol, P. Rosnet, J.-M. Rossignol

Laboratoire de Physique Corpusculaire, Université Blaise Pascal, IN^{2}P^3-CNRS, Clermont-Ferrand, 63177 Aubière, France

T. Fearnley, J.D. Hansen, J.R. Hansen, P.H. Hansen, B.S. Nilsson, B. Rensch, A. Wäänänen

Niels Bohr Institute, 2100 Copenhagen, Denmark[9]

G. Daskalakis, A. Kyriakis, C. Markou, E. Simopoulou, A. Vayaki

Nuclear Research Center Demokritos (NRCD), Athens, Greece

A. Blondel, J.C. Brient, F. Machefert, A. Rougé, M. Rumpf, A. Valassi,[6] H. Videau

Laboratoire de Physique Nucléaire et des Hautes Energies, Ecole Polytechnique, IN^{2}P^3-CNRS, 91128 Palaiseau Cedex, France

E. Focardi, G. Parrini, K. Zachariadou

Dipartimento di Fisica, Università di Firenze, INFN Sezione di Firenze, 50125 Firenze, Italy

R. Cavanaugh, M. Corden, C. Georgiopoulos, T. Huehn, D.E. Jaffe

Supercomputer Computations Research Institute, Florida State University, Tallahassee, FL 32306-4052, USA [13,14]

A. Antonelli, G. Bencivenni, G. Bologna,[4] F. Bossi, P. Campana, G. Capon, D. Casper, V. Chiarella, G. Felici, P. Laurelli, G. Mannocchi,[5] F. Murtas, G.P. Murtas, L. Passalacqua, M. Pepe-Altarelli

Laboratori Nazionali dell'INFN (LNF-INFN), 00044 Frascati, Italy

L. Curtis, S.J. Dorris, A.W. Halley, I.G. Knowles, J.G. Lynch, V. O'Shea, C. Raine, J.M. Scarr, K. Smith, P. Teixeira-Dias, A.S. Thompson, E. Thomson, F. Thomson, R.M. Turnbull

Department of Physics and Astronomy, University of Glasgow, Glasgow G12 8QQ,United Kingdom[10]

C. Geweniger, G. Graefe, P. Hanke, G. Hansper, V. Hepp, E.E. Kluge, A. Putzer, M. Schmidt, J. Sommer, K. Tittel, S. Werner, M. Wunsch

Institut für Hochenergiephysik, Universität Heidelberg, 69120 Heidelberg, Fed. Rep. of Germany[16]

R. Beuselinck, D.M. Binnie, W. Cameron, P.J. Dornan, M. Girone, S. Goodsir, E.B. Martin, P. Morawitz, A. Moutoussi, J. Nash, J.K. Sedgbeer, P. Spagnolo, A.M. Stacey, M.D. Williams

Department of Physics, Imperial College, London SW7 2BZ, United Kingdom[10]

V.M. Ghete, P. Girtler, D. Kuhn, G. Rudolph

Institut für Experimentalphysik, Universität Innsbruck, 6020 Innsbruck, Austria[18]

A.P. Betteridge, C.K. Bowdery, P. Colrain, G. Crawford, A.J. Finch, F. Foster, G. Hughes, R.W. Jones, T. Sloan, E.P. Whelan, M.I. Williams

Department of Physics, University of Lancaster, Lancaster LA1 4YB, United Kingdom[10]

C. Hoffmann, K. Jakobs, K. Kleinknecht, G. Quast, B. Renk, E. Rohne, H.-G. Sander, P. van Gemmeren, C. Zeitnitz

Institut für Physik, Universität Mainz, 55099 Mainz, Fed. Rep. of Germany[16]

J.J. Aubert, C. Benchouk, A. Bonissent, G. Bujosa, D. Calvet, J. Carr, P. Coyle, C. Diaconu, N. Konstantinidis, O. Leroy, F. Motsch, P. Payre, M. Talby, A. Sadouki, M. Thulasidas, A. Tilquin, K. Trabelsi

Centre de Physique des Particules, Faculté des Sciences de Luminy, IN^{2}P^3-CNRS, 13288 Marseille, France

M. Aleppo, F. Ragusa[12]

Dipartimento di Fisica, Università di Milano e INFN Sezione di Milano, 20133 Milano, Italy.

R. Berlich, W. Blum, V. Büscher, H. Dietl, G. Ganis, C. Gotzhein, H. Kroha, G. Lütjens, G. Lutz, W. Männer, H.-G. Moser, R. Richter, A. Rosado-Schlosser, S. Schael, R. Settles, H. Seywerd, R. St. Denis, H. Stenzel, W. Wiedenmann, G. Wolf

Max-Planck-Institut für Physik, Werner-Heisenberg-Institut, 80805 München, Fed. Rep. of Germany[16]

J. Boucrot, O. Callot,[12] S. Chen, A. Cordier, M. Davier, L. Duflot, J.-F. Grivaz, Ph. Heusse, A. Höcker, A. Jacholkowska, M. Jacquet, D.W. Kim,[2] F. Le Diberder, J. Lefrançois, A.-M. Lutz, I. Nikolic, M.-H. Schune, L. Serin, S. Simion, E. Tournefier, J.-J. Veillet, I. Videau, D. Zerwas

Laboratoire de l'Accélérateur Linéaire, Université de Paris-Sud, IN^{2}P^3-CNRS, 91405 Orsay Cedex, France

P. Azzurri, G. Bagliesi, S. Bettarini, C. Bozzi, G. Calderini, V. Ciulli, R. Dell'Orso, R. Fantechi, I. Ferrante, A. Giassi, A. Gregorio, F. Ligabue, A. Lusiani, P.S. Marrocchesi, A. Messineo, F. Palla, G. Sanguinetti, A. Sciabà, J. Steinberger, R. Tenchini, C. Vannini, A. Venturi, P.G. Verdini

Dipartimento di Fisica dell'Università, INFN Sezione di Pisa, e Scuola Normale Superiore, 56010 Pisa, Italy

G.A. Blair, L.M. Bryant, J.T. Chambers, Y. Gao, M.G. Green, T. Medcalf, P. Perrodo, J.A. Strong, J.H. von Wimmersperg-Toeller

Department of Physics, Royal Holloway & Bedford New College, University of London, Surrey TW20 OEX, United Kingdom[10]

D.R. Botterill, R.W. Clifft, T.R. Edgecock, S. Haywood, P. Maley, P.R. Norton, J.C. Thompson, A.E. Wright

Particle Physics Dept., Rutherford Appleton Laboratory, Chilton, Didcot, Oxon OX11 OQX, United Kingdom[10]

B. Bloch-Devaux, P. Colas, B. Fabbro, W. Kozanecki, E. Lançon, M.C. Lemaire, E. Locci, P. Perez, J. Rander, J.-F. Renardy, A. Rosowsky, A. Roussarie, J.-P. Schuller, J. Schwindling, A. Trabelsi, B. Vallage

CEA, DAPNIA/Service de Physique des Particules, CE-Saclay, 91191 Gif-sur-Yvette Cedex, France[17]

S.N. Black, J.H. Dann, H.Y. Kim, A.M. Litke, M.A. McNeil, G. Taylor

Institute for Particle Physics, University of California at Santa Cruz, Santa Cruz, CA 95064, USA[19]

C.N. Booth, R. Boswell, C.A.J. Brew, S. Cartwright, F. Combley, M.S. Kelly, M. Lehto, W.M. Newton, J. Reeve, L.F. Thompson

Department of Physics, University of Sheffield, Sheffield S3 7RH, United Kingdom[10]

K. Affholderbach, A. Böhrer, S. Brandt, G. Cowan, J. Foss, C. Grupen, P. Saraiva, L. Smolik, F. Stephan

Fachbereich Physik, Universität Siegen, 57068 Siegen, Fed. Rep. of Germany[16]

M. Apollonio, L. Bosisio, R. Della Marina, G. Giannini, B. Gobbo, G. Musolino

Dipartimento di Fisica, Università di Trieste e INFN Sezione di Trieste, 34127 Trieste, Italy

J. Putz, J. Rothberg, S. Wasserbaech, R.W. Williams

Experimental Elementary Particle Physics, University of Washington, WA 98195 Seattle, U.S.A.

S.R. Armstrong, E. Charles, P. Elmer, D.P.S. Ferguson, S. González, T.C. Greening, O.J. Hayes, H. Hu, S. Jin, P.A. McNamara III, J.M. Nachtman, J. Nielsen, W. Orejudos, Y.B. Pan, Y. Saadi, I.J. Scott, J. Walsh, Sau Lan Wu, X. Wu, J.M. Yamartino, G. Zobernig

Department of Physics, University of Wisconsin, Madison, WI 53706, USA[11]

[1]Now at Princeton University, Princeton, NJ 08544, U.S.A.

[2]Permanent address: Kangnung National University, Kangnung, Korea.

[3]Also at Dipartimento di Fisica, INFN Sezione di Catania, Catania, Italy.

[4]Also Istituto di Fisica Generale, Università di Torino, Torino, Italy.

[5]Also Istituto di Cosmo-Geofisica del C.N.R., Torino, Italy.

[6]Supported by the Commission of the European Communities, contract ERBCHBICT941234.

[7]Supported by CICYT, Spain.

[8]Supported by the National Science Foundation of China.

[9]Supported by the Danish Natural Science Research Council.

[10]Supported by the UK Particle Physics and Astronomy Research Council.

[11]Supported by the US Department of Energy, grant DE-FG0295-ER40896.

[12]Also at CERN, 1211 Geneva 23,Switzerland.

[13]Supported by the US Department of Energy, contract DE-FG05-92ER40742.

[14]Supported by the US Department of Energy, contract DE-FC05-85ER250000.

[15]Permanent address: Universitat de Barcelona, 08208 Barcelona, Spain.

[16]Supported by the Bundesministerium für Bildung, Wissenschaft, Forschung und Technologie, Fed. Rep. of Germany.

[17]Supported by the Direction des Sciences de la Matière, C.E.A.

[18]Supported by Fonds zur Förderung der wissenschaftlichen Forschung, Austria.

[19]Supported by the US Department of Energy, grant DE-FG03-92ER40689.

[20]Now at School of Operations Research and Industrial Engineering, Cornell University, Ithaca, NY 14853-3801, U.S.A.

[21]Now at Schweizerischer Bankverein, Basel, Switzerland.

1 Introduction

The main consequence of supersymmetric theories [1] is the doubling of the particle spectrum: for each fermion's chirality state a scalar particle is introduced. Depending on the chirality state they are associated to, the scalar partners of the leptons (sleptons) are called "right" ($\tilde{\ell}_R$) or "left" ($\tilde{\ell}_L$). These are the eigenstates of the weak interaction. Particle masses are generated by the Higgs mechanism with two doublets. The partners of the Higgs and gauge bosons are the Higgsinos and gauginos. Exact supersymmetry implies mass degeneracy for the particles and their supersymmetric partners; since no evidence for supersymmetry has been observed up to now, supersymmetry has to be a broken symmetry. When supersymmetry is broken, the weak eigenstates mix to form the mass eigenstates: neutral Higgsinos and gauginos mix to form the mass eigenstates called "neutralinos", and the charged Higgsinos and gauginos mix to form the eigenstates called "charginos".

In order to preserve one of the most appealing aspects of supersymmetry, i.e., possibly being a solution to the hierarchy problem, supersymmetric particles must have masses of order TeV/c^2 or less. The increase of the centre–of–mass energy of LEP, CERN's large e^+e^- collider, to 140 GeV in 1995 and above the W pair production threshold in 1996 has opened a new energy regime to be probed in search for supersymmetry [2, 3, 4]. In this letter the results of a search for the scalar partners of the leptons at centre–of–mass energies from 161 GeV to 172 GeV in the data recorded by the ALEPH detector in 1996 are presented.

The minimal supersymmetric extension of the standard model (MSSM) [1] is used as a reference model. R–parity, a quantum number that distinguishes standard model particles from supersymmetric particles [5], is assumed to be conserved, implying that sleptons can only be produced in pairs. In general the sleptons decay to their standard model partner and the lightest neutralino (χ) with an undetectable lifetime. The latter is assumed to be stable and escapes the apparatus undetected, leading to a final state of acoplanar lepton pairs. In the following, any deviation from this behaviour will be mentioned explicitly.

The only dependence of the cross section for smuon ($\tilde{\mu}$) and stau ($\tilde{\tau}$) production on supersymmetric parameters is through the slepton mass matrix. The production proceeds via s channel only, whereas selectrons ($\tilde{\mathrm{e}}$) can also be produced by exchanging neutralinos in the t channel. The selectron cross section [6] therefore depends on the selectron mass and, via the t channel, on the MSSM parameters (the supersymmetric Higgs mass term μ, the soft supersymmetry breaking term associated to the $SU(2)_L$ group M_2, and the ratio of the vacuum expectation values of the two Higgs doublets, $\tan\beta$).

The off-diagonal elements of a slepton mass matrix are proportional to the lepton's mass, therefore left and right sleptons can mix to form the mass eigenstates. However, mixing is expected to be negligible for smuons and selectrons due to the small masses of their standard model partners.

The unification condition $M_1 = \frac{5}{3}\tan^2\vartheta_W M_2$, where M_1 is the soft supersymmetry breaking parameter associated with the $U(1)_Y$ group, is assumed to be valid. In the following, the parameter space where $|\mu| \gg M_2$ ($|\mu| \ll M_2$) will be referred to as the "gaugino" ("higgsino") region, as suggested by the field content of the lightest neutralino.

1.1 The ALEPH Detector

The ALEPH detector is described in detail in Ref. [7]. An account of the performance of the detector and a description of the standard analysis algorithms can be found in Ref. [8]. Here, only a brief description of the detector elements and the algorithms relevant for this analysis is given.

In ALEPH, the trajectories of charged particles are measured with a silicon vertex detector, a cylindrical drift chamber, and a large time projection chamber (TPC). These detector components are located in a 1.5 T magnetic field provided by a superconducting solenoidal coil. The electromagnetic calorimeter (ECAL), placed between the TPC and the coil, is a highly segmented sampling calorimeter which is used to identify electrons and photons and to measure their energy and position. The luminosity monitors (LCAL and SICAL) extend the calorimetric coverage down to 30 mrad from the beam axis, taking into account the additional shielding against beam related background, installed prior to the 1996 running. The hadron calorimeter (HCAL) consists of the iron return yoke of the magnet instrumented with streamer tubes. It provides a measurement of hadronic energy and, together with the external muon chambers, muon identification.

Global event quantities are measured with an energy flow algorithm. This algorithm combines individual calorimeter and tracker measurements into energy flow "objects". These objects are classified as photons, neutral hadrons, and charged particles.

The present analysis makes use of lepton identification. In ALEPH, electrons are identified by the longitudinal and the transverse energy distribution of the ECAL shower, and by the specific ionization information in the TPC when available [8]. Muons are identified through their hit pattern in the HCAL and associated hits in the muon chambers.

1.2 Data Sample

For this analysis, the data taken in 1996 at centre–of–mass energies of 161.3, 170.3 and 172.3 GeV are used, which correspond to integrated luminosities of 11.1 pb^{-1}, 1.1 pb^{-1} and 9.5 pb^{-1} respectively. In the following, these three centre–of–mass energies will be referred to as 161 and 172 GeV, combining the two points at 170.3 and 172.3 GeV. Since the expected limits for sleptons are still in the kinematic reach of the 5.7 pb^{-1} data taken at centre–of–mass energies of 130 and 136 GeV in 1995, the results published in [4] are combined with the results of the present analysis for the 161 and 172 GeV data.

1.3 Monte Carlo Sample

Samples of all the major background processes corresponding to at least 20 times the collected luminosity have been generated. The most important background sources are lepton pair production, $\gamma\gamma$ collisions with lepton production, W pair production, $Z\gamma^*$ production (where γ^* denotes a virtual Z or photon), Zee and $We\nu$ production. Bhabha processes were simulated with UNIBAB [9], muon and tau pair production with KORALZ [10], $\gamma\gamma$ processes with PHOT02 [11] ($\gamma\gamma \to$ leptons) and PYTHIA [12] ($\gamma\gamma \to$ hadrons), WW production with KORALW [13], and the remaining four–fermion processes with PYTHIA. An additional potential source of background may arise from $\nu\bar{\nu}\gamma$ events in which the photon converts. This background was generated with KORALZ.

The signal was generated using SUSYGEN [14] with final state radiation added by the PHOTOS [15] package and tau decays simulated with TAUOLA [16]. A full simulation of the detector was used for the background and the signal for some parameter sets, and a fast simulation for interpolation of the signal efficiencies.

2 Searches

Slepton pair production leads to a final state characterised by leptons of the same flavour. These leptons are acoplanar with the beam due to the missing energy and momentum carried away by the χ's.

Several searches have been developed depending on the flavour of the leptons and the mass difference between the slepton and the χ. The main backgrounds for large mass differences are W pair production, four–fermion processes and dilepton production, whereas for small mass differences the dominant background comes from two–photon processes with lepton production. Therefore, one set of selections has been designed for large mass differences (Section 2.1), and an additional analysis was optimised for mass differences of about 5 GeV/c^2 (Section 2.2) in the case of smuons and selectrons.

The cuts are described in this section and listed in Table 1. The positions of the most important cuts are determined using the $\bar{N}_{95}$ prescription advocated in [17], i.e., minimising the cross section expected to be excluded on average in the absence of a signal.

The definition of a good charged track as originating from within a cylinder of 1 cm radius and 10 cm length, which is centred on the nominal interaction point and parallel to the beam axis, having at least four TPC hits, a momentum greater than $0.5\%\sqrt{s}$ and a minimum polar angle of 18.2° is common to all analyses.

For selectrons and smuons, events are required to have two good charged tracks with opposite electric charges. To search for staus, all charged and neutral objects of an event are clustered into two jets using the Durham algorithm, as in a large fraction of tau decays neutral particles are produced. After having identified photon conversions with a standard pair finding algorithm [8], one jet is required to consist of exactly one good charged track, whereas the other is allowed to have one, two or three charged tracks. The vector sum of the momenta of these tracks will be referred to as a single track for simplicity.

To avoid selecting events with a single converted photon, the acollinearity, defined as the angle between the track momenta, should be greater than 2°. The background coming from tagged two–photon processes is eliminated by requiring that no energy be reconstructed in a cone of 12° around the beam axis (corresponding to an effective threshold of 90 MeV). This requirement introduces an inefficiency due to beam related background and detector noise, which was measured to be 4% (2%) at centre–of–mass energy of 161 (172) GeV, using events triggered at random beam crossings.

Table 1: Selection criteria.

	selectron $\tilde{\mathrm{e}}$**, smuon** $\tilde{\mu}$ $M_{\tilde{\ell}} - M_\chi > 6$ GeV/c^2	$M_{\tilde{\ell}} - M_\chi \leq 6$ GeV/c^2	**stau** $\tilde{\tau}$
charged tracks	two identified leptons (e, μ, τ)		
neutral veto	yes	no cut	yes
acollinearity	$\alpha > 2°$		
acoplanarity	$\Phi_{\mathrm{aco}} < 170°$		
visible mass	$M_{\mathrm{vis}} > 4$ GeV/c^2	$M_{\mathrm{vis}} < 20\%\sqrt{s}$	$M_{\mathrm{vis}} > 6$ GeV/c^2
energy in 12°	$E_{12} = 0$		
missing momentum	$p_{\mathrm{T}} > 3\%\sqrt{s}$	$p_{\mathrm{T}} > 1\%\sqrt{s}$ $p < 10\%\sqrt{s}$ $\lvert\cos\theta\rvert < 0.90$	if $M_{\mathrm{vis}} < 30$ GeV/c^2 then $p_{\mathrm{T}} > 6\%\sqrt{s}$ $\lvert\cos\theta\rvert < 0.866$
ρ	$\rho > 2$ GeV/c	$\rho > 1$ GeV/c	$17.1\rho + 120 - \Phi_{\mathrm{aco}} > 0$
lepton momenta p_1, p_2	$p_1, p_2 > 0.5\%\sqrt{s}$	$p_{T1}, p_{T2} > 0.5\%\sqrt{s}$ $p_1, p_2 < 10\%\sqrt{s}$	$p_1, p_2 > 0.5\%\sqrt{s}$ $\min(p_1, p_2) < 15$ GeV/c
$\sqrt{s}$ =161 GeV	$p_1, p_2 < 75$ GeV/c		$p_1, p_2 < 30$ GeV/c
$\sqrt{s}$ =172 GeV	$p_1, p_2 < 80$ GeV/c		$p_1, p_2 < 22$ GeV/c
χ_{WW}			
$\sqrt{s}$ =161 GeV	$\chi_{\mathrm{WW}} > 0.5$		
$\sqrt{s}$ =172 GeV	$\chi_{\mathrm{WW}} > 2.0$		
Fisher variable		$y > -15$	

2.1 Large Mass Differences

To reject radiative fermion pair production with an initial state radiation photon in the detector while avoiding to veto τ decays and signal events with final state radiation, a neutral veto is applied if three conditions are fulfilled simultaneously: a neutral energy flow object of more than 4 GeV is reconstructed, its angle with each of the two tracks is greater than 10° and its invariant mass with each of the two tracks is greater than 2 GeV/c^2.

2.1.1 Selectrons and Smuons

In order to reject events from fermion pair production, the acoplanarity angle Φ_{aco} of the two tracks is required to be less than 170°. The acoplanarity is defined as the angle between the track momenta projected onto a plane perpendicular to the beam axis. To reject the remaining eeγ events, the energy of the tracks, including neutral objects in a cone of 10° around either track, is required to be less than 75 (80) GeV at centre–of–mass energy of 161 (172) GeV.

The (non–WW) four–fermion and two–photon backgrounds are reduced by demanding that the visible mass be greater than 4 GeV/c^2. The untagged two–photon processes are reduced further by demanding that the missing transverse momentum p_T of the event (Fig. 1a) be greater than $3\%\sqrt{s}$. Remaining two–photon events ($\gamma\gamma \to \tau\tau$) are reduced by the following procedure: the track momenta are projected onto a plane transverse to the beam axis and the thrust axis is calculated from the projected momenta. The scalar sum ρ of the transverse components of the projected momenta with respect to this thrust axis is required to be greater than 2 GeV/c.

At this point of the analysis, only the background from W pair production, where both W's decay leptonically, has to be dealt with. In only two out of nine cases the W's are expected to decay to two electrons or two muons. Therefore two identified electrons (muons) are required for the selectron (smuon) search.

The cuts described so far are common to both centre–of–mass energies. The cross section for W pair production, however, increases almost by a factor of four going from 161 GeV to 172 GeV. Therefore more stringent cuts are applied in the latter case.

For leptons from W pair production, a lepton energy of roughly $\sqrt{s}/4$ smeared with the boost and width of the W is expected. Therefore the variable

$$\chi_{\mathrm{WW}} = \frac{1}{2}\sum_{i=1}^{2}\left(\frac{E_i - \sqrt{s}/4}{6\ \mathrm{GeV}}\right)^2$$

is defined, where E_i are the lepton energies and 6 GeV is the expected energy spread. For the W background this variable peaks near zero while for a signal not too similar to a W it is expected to be flatter (Fig. 1b). At 161 GeV, $\chi_{\mathrm{WW}} > 0.5$ is required. This cut is tightened to $\chi_{\mathrm{WW}} > 2$ at 172 GeV to cope with the higher W cross section and the broader distribution of the lepton momenta. It is not applied for $M_{\tilde{\ell}} > 70$ GeV/c^2 to save efficiency. The point of the transition was determined with the $\bar{N}_{95}$ procedure. After these cuts the residual WW background is still much higher at 172 GeV than at 161 GeV. In order to reduce the background even further at 172 GeV, it is required that the lepton momenta must fall in the range kinematically allowed for the specific combination of slepton and χ masses. Typical efficiencies and background expectations for $\tilde{\ell}_R\tilde{\ell}_R$ production for these searches are listed in Table 2.

2.1.2 Staus

Background from untagged two–photon processes is efficiently suppressed by requiring a missing transverse momentum of at least $6\%\sqrt{s}$, if the visible mass of the event is less than 30 GeV/c^2. Events from fermion pair production and two–photon processes are rejected by a two–dimensional cut in ρ and Φ_{aco} (defined as before, but using jets instead of track momenta): (ρ,Φ_{aco}) is not allowed in the triangular region $(0, 120)$ - $(3.5, 180)$ - $(0, 180)$. Furthermore the jet masses are required to be less than 8 GeV/c^2. Remaining difermion events with an ISR photon undetected in the beam pipe are suppressed by requiring a polar angle of the missing momentum of at least 30°.

After requiring a minimum visible mass of 6 GeV/c^2, the remaining background predominantly consists of events from W pair production. As the leptons from W bosons decaying into electrons or muons are in general more energetic than leptons from τ decays, cuts are applied on the momenta of identified electrons or muons (including all neutral objects within 10°). At $\sqrt{s}$ = 161 (172) GeV, the leading lepton is required to have a momentum p_1 less than 30 (22) GeV/c (Fig. 1c). In case a second lepton is found in the event, its momentum is required to be less than 15 GeV/c.

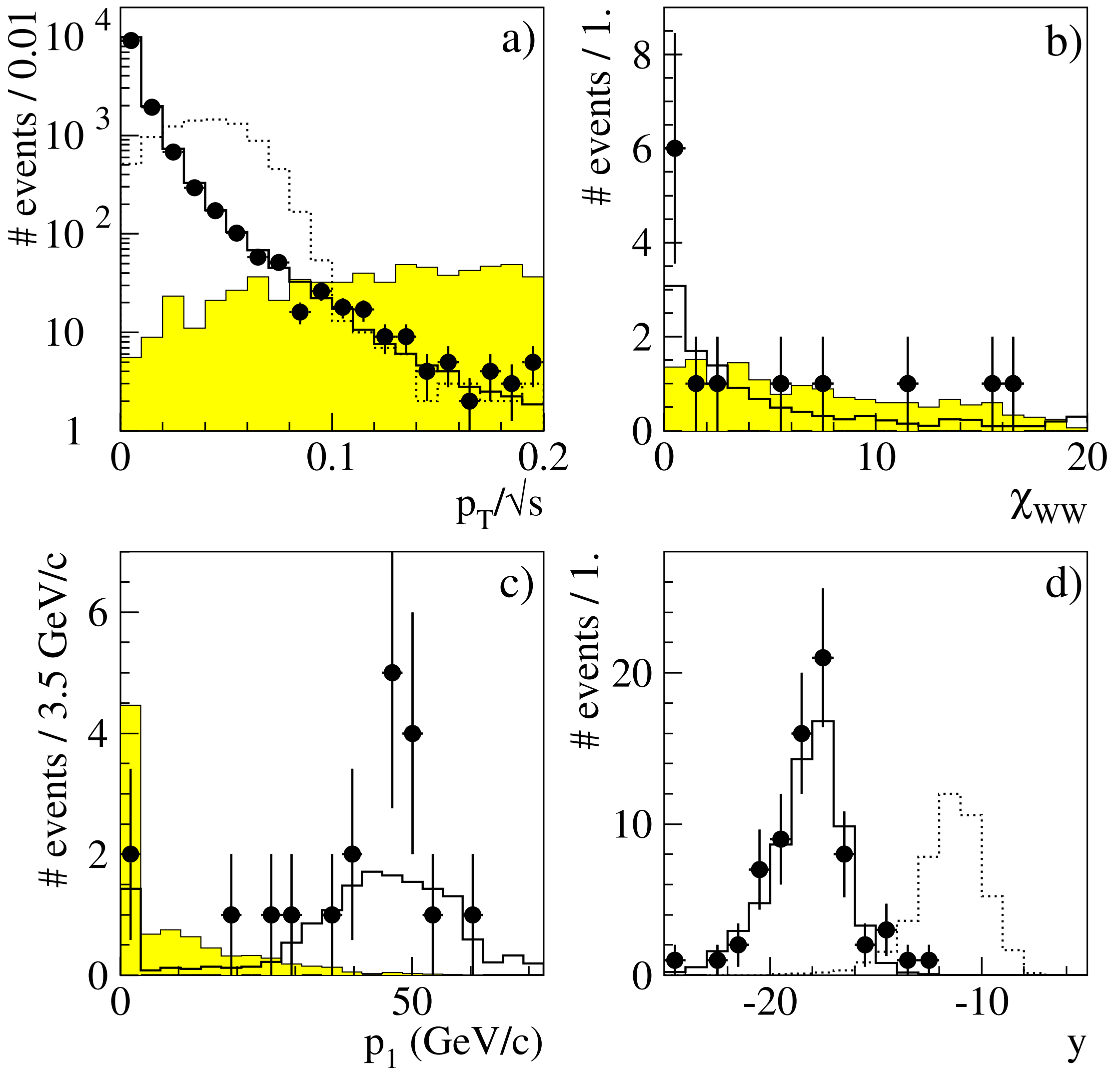

Figure 1: Distributions of a) the missing transverse momentum, b) the χ_{WW} variable for the selectrons and smuons, c) the momentum of the leading lepton p_1 as used in the stau search, d) the Fisher variable. The points are the data (161 GeV and 172 GeV combined), the open histograms the background Monte Carlo normalised to the recorded luminosity, the shaded histograms a signal with a mass difference of 30 GeV$/c^2$ in arbitrary normalisation, and the dotted histograms in plots a) and d) are signal histograms with a mass difference of 5 GeV$/c^2$. In order to preserve sufficient statistics only subsets of the cuts on the other variables were applied for these plots.

After these cuts a total background of 0.5 (1) events is expected at 161 (172) GeV. Examples of the efficiencies to select stau events are presented in Table 2.

2.2 Small Mass Differences

The analysis described in this section is optimised for small mass differences. It is used for mass differences less than 6 GeV$/c^2$. The background from fermion pair production and four–fermion processes is rejected by demanding a maximum lepton momentum of $10\%\sqrt{s}$, a visible mass smaller than $20\%\sqrt{s}$, a missing momentum of the event smaller

Table 2: Signal cross sections $\sigma_{\tilde{\ell}_R}$ ($\tan\beta = 2$, $\mu = -200$ GeV/c^2 for $\tilde{e}_R$), efficiencies ϵ and background cross sections σ_B for slepton searches. For simplicity, the background is given for each mass combination separately in spite of the overlap among the various rows.

$\sqrt{s}$ (GeV)	Slepton	$M_{\tilde{\ell}}$ (GeV/c^2)	M_χ (GeV/c^2)	$\sigma_{\tilde{\ell}_R}$ (fb)	ϵ (%)	σ_B (fb)
161	$\tilde{e}$	75	0	238	58	60
		75	30	160	58	60
		75	70	38	45	35
		75	72.5	34	9	35
	$\tilde{\mu}$	55	0	401	66	43
		55	30		61	43
		55	50		54	35
		55	52.5		18	35
	$\tilde{\tau}$	50	0	514	39	43
		50	25		40	43
172	$\tilde{e}$	75	0	619	67	117
		75	30	415	67	91
		75	70	107	45	35
		75	72.5	97	9	35
	$\tilde{\mu}$	55	0	411	60	93
		55	30		55	54
		55	50		54	35
		55	52.5		18	35
	$\tilde{\tau}$	50	0	502	37	93
		50	25		36	93

than $10\%\sqrt{s}$ and the acoplanarity angle of the two leptons to be below $170°$.

Since the signal resembles the two–photon background, the cuts are less stringent than in the large mass difference selection. The missing transverse momentum is required to exceed $1\%\sqrt{s}$ (Fig. 1a), ρ is required to be greater than 1 GeV/c and the visible mass is required to be greater than 4 GeV/c^2. The cosine of the polar angle of the missing momentum must be less than 0.9 and the transverse momentum of each lepton greater than $0.5\%\sqrt{s}$.

In order to reduce the large $\gamma\gamma$–background a Fisher discriminant analysis [18] has been used. This method exploits the remaining modest differences between $\gamma\gamma$–events and the signal, taking into account the correlations among the variables used. For this analysis, the visible event mass, the missing transverse momentum, the missing momentum along the beam direction, the variable ρ, the maximum and minimum lepton transverse momenta and the acollinearity are used to calculate the Fisher variable y (Fig. 1d). For $y > -15$, the cut chosen by means of the $\bar{N}_{95}$ procedure, 98% of the remaining background is rejected, whereas about 98% of a signal with a mass difference of 5 GeV/c^2 is kept. After these cuts a total background of 1 (1) event is expected in the whole data sample for selectrons (smuons).

3 Results

Three candidates are observed in the large mass difference analyses and are listed in Table 3. The selectron candidate at 161 GeV can be either interpreted as a WW event, where the first electron originates from the W decay and the second from a cascade decay W to τ to electron, or as a $Z\gamma^*$ event with the Z decaying to neutrinos, since the recoil mass to the electron pair is 90 GeV/c^2. The decay products of the stau candidate, observed at 161 GeV, are consistent with the masses of the ρ and a_1 mesons. From the decay kinematics an upper limit on the tau energy of 22 GeV can be inferred. Therefore it is unlikely that this is a WW event, but it is compatible with $Z\gamma^*$. One smuon candidate is observed at 172 GeV. The recoil mass is 130 GeV/c^2, so that the WW (cascade decays to muons via taus) and the $Z\gamma^*$ hypotheses are possible explanations.

In the analysis optimised for small mass difference five candidates compatible with $\gamma\gamma$ and WW production are observed and listed also in Table 3.

Table 3: Kinematic properties of the candidate events.

$\sqrt{s}$ (GeV)	Slepton	$M_{\tilde{\ell}} - M_\chi$ (GeV/c^2)	p_1 (GeV/c)	p_2 (GeV/c)	event p_{T} GeV/c
161	$\tilde{\mathrm{e}}$	> 6	44.1	12.0	23.1
	$\tilde{\tau}$		11.2	9.7	10.6
172	$\tilde{\mu}$		19.4	17.4	22.8
161	$\tilde{\mu}$	≤ 6	3.9	2.4	3.1
172	$\tilde{\mu}$		6.2	2.7	4.8
			8.0	1.9	4.5
	$\tilde{\mathrm{e}}$		16.7	1.8	10.7
			6.9	5.9	2.6

To summarise, in the $(M_{\tilde{\ell}}, M_\chi)$ plane, for $M_{\tilde{\ell}}$ greater than 45 GeV/c^2, eight events are selected in the data in agreement with the seven events expected from standard model processes. In the absence of a signal, limits are set for various processes.

Limits

The limits are derived from the present results combined with the ALEPH results from LEP1.5 [4], obtained at $\sqrt{s} = 130 - 136$ GeV/c^2. For each combination of slepton and neutralino masses only the candidates that fulfil the kinematic requirements of the specific combination are taken into account in the calculation of the limit. Systematic uncertainties are taken into account by reducing the expected number of signal events by one standard deviation. The main contributions to the total systematic error ($\sim 3\%$) come from Monte Carlo statistics, the luminosity measurement ($< 1\%$) and lepton identification efficiencies ($\sim 2\%$).

For smuons and staus, fewer assumptions are necessary to derive a mass limit than for selectrons, for which the t channel production requires specification of the neutralino

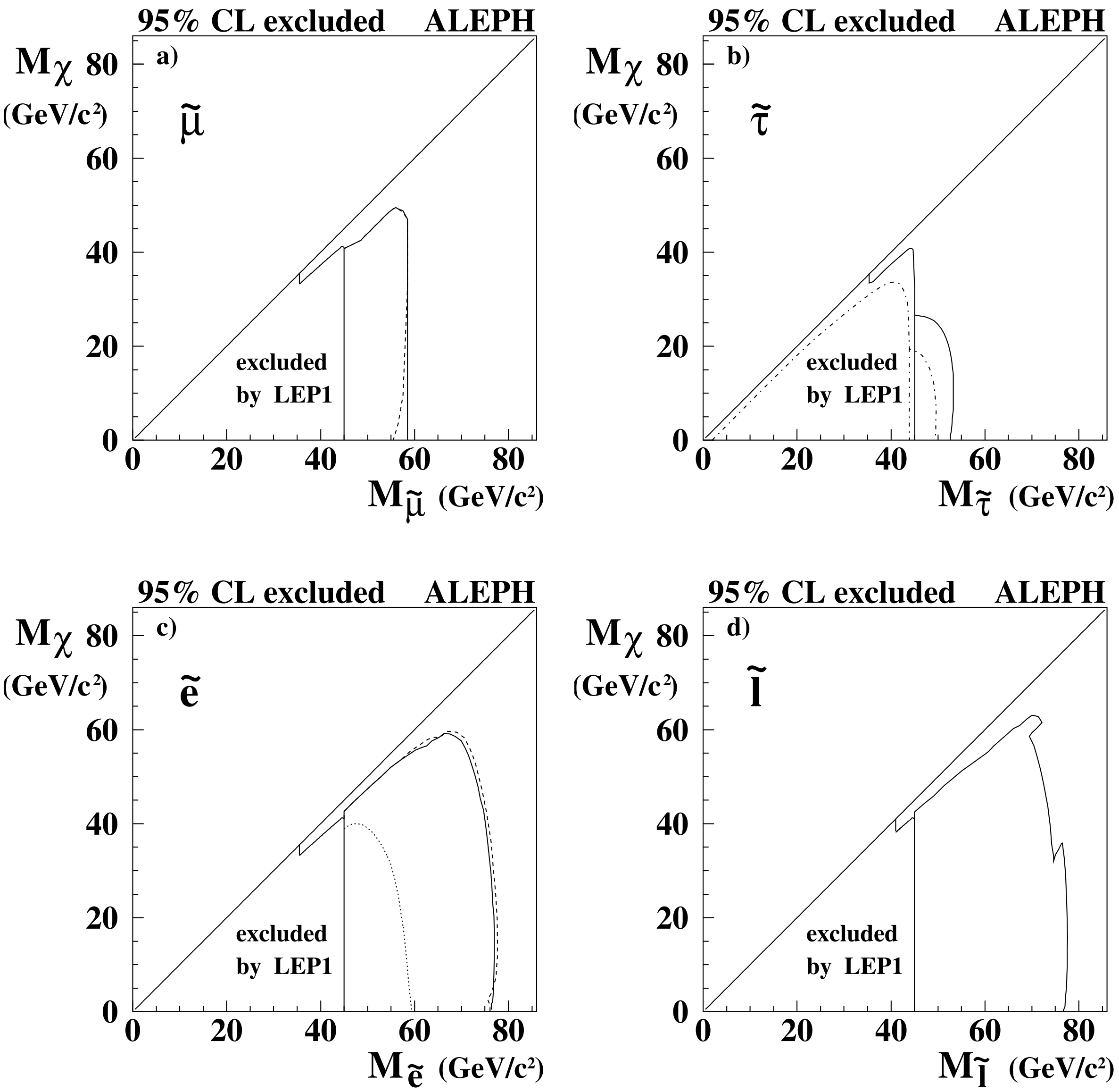

Figure 2: a) The solid curve shows the limit obtained for $\tilde{\mu}_R$ assuming BR($\tilde{\mu}_R \to \mu\chi$) = 100% and the dashed curve shows the effect of cascade decays for $\mu = -200$ GeV/c^2 and $\tan\beta = 2$, assuming no efficiency for the cascade decays. b) Mass limits for $\tilde{\tau}_R$ (solid curve) and a mixed state $\tilde{\tau}_1$ decoupled from the Z (dash–dotted curve), assuming BR($\tilde{\tau} \to \tau\chi$) = 100%. c) $\tilde{\mathrm{e}}_R$ mass limit for $\tan\beta = 2$. The solid curve shows the limit for the case $\mu = -200$ GeV/c^2, the dashed curve for $\mu = 1000$ GeV/c^2 assuming no efficiency for cascade decays. The dotted curve is the LEP 1.5 limit. d) $\tilde{\mathrm{e}}_R$ and $\tilde{\mu}_R$ limits, combined assuming mass degeneracy and including the effect of cascade decays for $\tan\beta = 2$ and $\mu = -200$ GeV/c^2.

parameters. Unless stated otherwise, limits are derived under the assumption that only $\tilde{\ell}_R\tilde{\ell}_R$ production contributes. This assumption is conservative because of the smaller cross section for the production of right-handed sleptons compared to left-handed sleptons for pure s channel production.

Using the limit on additional contributions to the invisible width of the Z as derived with the full LEP1 statistics [19] (sleptons do not contribute to the leptonic width, since they fail the cut on the acollinearity in the standard analysis), lower limits on slepton masses can be set independent of the neutralino mass. For a single right-handed slepton this corresponds to 35 GeV/c^2. Assuming all three right-handed sleptons to be degenerate in mass, slepton masses below 41 GeV/c^2 are excluded.

The limit on the $\tilde{\mu}_R$ is shown in Figure 2a. Smuon masses up to 59 GeV/c^2 are excluded for mass differences to the lightest neutralino greater than 10 GeV/c^2. This limit is reduced when cascade decays via heavier neutralinos are taken into account. Conservatively no efficiency is assumed for these decays. The dashed curve shows this effect for $\mu = -200$ GeV/c^2 and $\tan\beta = 2$ as an example.

Mixing is expected to be negligible for all sleptons except for staus, since the tau is much heavier than the other leptons. Therefore limits are calculated for staus in mixed and unmixed scenarios. Assuming mixing effects to be negligible, the most conservative limits are set by considering pair production of $\tilde{\tau}_R$ (Fig. 2b, solid curve). In the case where $\tilde{\tau}_L$ and $\tilde{\tau}_R$ mix, limits are set on the mass of the lightest stau $\tilde{\tau}_1$, choosing the mixing angle such that $\tilde{\tau}_1$ completely decouples from the Z boson (Fig. 2b, dash–dotted curve). For this purpose the search for staus at LEP1 [20] is updated with the full LEP1 statistics and included in the determination of the limit. For a mass difference between stau and neutralino of more than 30 GeV/c^2, the $\tilde{\tau}_R$ ($\tilde{\tau}_1$) with mass less than 53 GeV/c^2 (47 GeV/c^2) is excluded.

Limits for the selectrons are obtained in the gaugino region, where the cross section is enhanced due to the t channel contribution. The limits are shown in Fig. 2c using two different values of μ (1000 GeV/c^2 and -200 GeV/c^2) for $\tan\beta = 2$. The accessible region for the candidate of the large mass difference selection and one of the candidates of the small mass difference selection is entirely excluded. The actual limit is in a region of the ($M_{\tilde{e}}, M_\chi$) plane where only one candidate in the small mass difference domain must be considered. Cascade decays are taken into account according to the branching ratio $\tilde{e} \to e\chi$ for the particular choice of the MSSM parameters, assuming no efficiency for cascades. This leads to a degradation of the selectron mass limit for small M_χ. The effect of cascade decays is not as pronounced as for the smuons due to the increasing cross section for small neutralino masses. The limit shown in Fig. 2c is extended by the single photon counting measurements to 80 GeV/c^2 for neutralino masses less than 10 GeV/c^2 [21] under the assumption of degenerate left and right selectrons at 90% confidence level.

A limit on $M_{\tilde{\ell}}$ is derived assuming degeneracy of the three flavours. The highest sensitivity in the direct search is reached when only selectrons and smuons are combined, since staus are selected with similar background but lower efficiency. The result for $\tan\beta = 2$ and $\mu = -200$ GeV/c^2 is shown in Fig. 2d. Only $\tilde{\ell}_R\tilde{\ell}_R$ production is considered. The smuon candidate of the large mass difference selection causes a notch in the limit curve.

Assuming scalar mass unification (m_0) at the GUT scale there is a relation among the

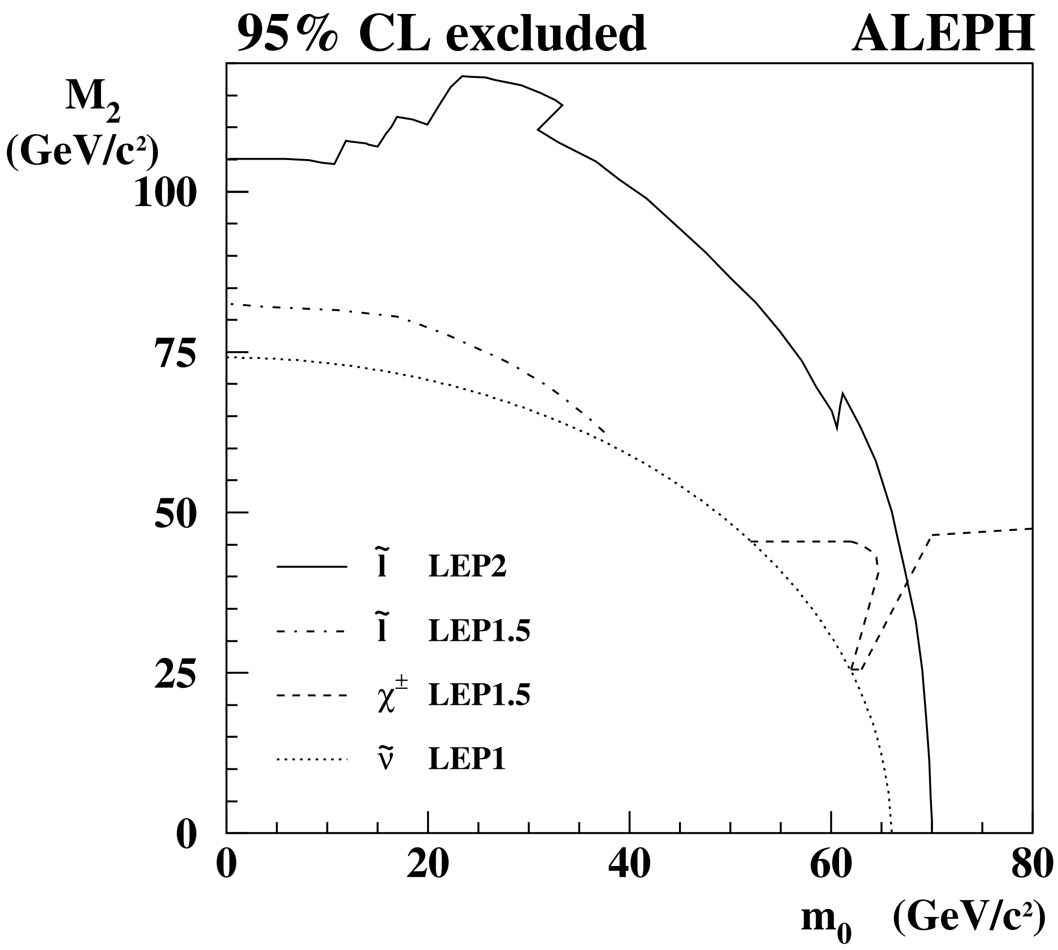

Figure 3: Limit in the (m_0, M_2) plane combining selectrons and smuons for $\tan\beta = 2$ and $\mu = -200$ GeV$/c^2$ (solid curve). The dotted curve shows the sneutrino limit (43 GeV$/c^2$) from LEP1, the dashed curve shows the gain in exclusion due to the chargino limit from LEP1.5 and the dash–dotted curve shows the slepton limit of LEP1.5.

masses of the scalar particles at the electroweak scale [22]. In particular, for sleptons one obtains:

$$
\begin{aligned}
M^2_{\tilde{\ell}_R} &= m_0^2 + 0.22 M_2^2 - \sin^2\vartheta_W M_Z^2 \cos 2\beta \\
M^2_{\tilde{\ell}_L} &= m_0^2 + 0.75 M_2^2 - 0.5(1 - 2\sin^2\vartheta_W) M_Z^2 \cos 2\beta \\
M^2_{\tilde{\nu}} &= m_0^2 + 0.75 M_2^2 + 0.5 M_Z^2 \cos 2\beta
\end{aligned}
$$

In the case of the staus, mixing plays a role for large values of $\tan\beta$ and/or μ. Depending on the masses of left- and right-handed sleptons, additional production channels like $\tilde{e}_R\tilde{e}_L$ and $\tilde{\ell}_L\tilde{\ell}_L$ may be open leading to a higher total cross section. Again, the highest sensitivity is obtained when only selectrons and smuons are used for the combination. The excluded region in the (m_0, M_2) plane for $\tan\beta = 2$ and $\mu = -200$ GeV$/c^2$ is shown in Fig. 3. The notch for intermediate values of m_0 comes from the smuon candidate of the large mass difference selection, and the structures for small m_0 come from the various small mass difference candidates. For small M_2, i.e., small neutralino masses, the processes $\tilde{\ell}_L\tilde{\ell}_L$ and $\tilde{e}_L\tilde{e}_R$ improve only by about 1 GeV/c^2 the limit of degenerate $\tilde{\ell}_R$ because of the high branching ratio of $\tilde{\ell}_L$ to charginos, which dominantly decay hadronically in this region. While the limit on the sneutrino mass at LEP 1 still improved the limit at LEP 1.5, this is not the case anymore.

4 Conclusions

In data samples of 11.1 pb^{-1} and 10.7 pb^{-1} recorded in 1996 by the ALEPH detector at LEP at centre–of–mass energies of 161 GeV and 172 GeV, searches for signals of scalar lepton production have been performed. The number of candidate events observed is consistent with the background expected from four–fermion processes and $\gamma\gamma$–interactions. The following limits have been set at 95% confidence level ($\mu = -200$ GeV/c^2 and $\tan\beta = 2$, where relevant):

- 59 GeV/c^2 for right smuons when $M_{\tilde{\mu}_R} - M_\chi$ is greater than 10 GeV/c^2,
- 53 GeV/c^2 for right staus if M_χ is smaller than 20 GeV/c^2,
- 75 GeV/c^2 for selectrons when $M_{\tilde{e}_R} - M_\chi$ is greater than 35 GeV/c^2, taking cascade decays into account,
- 58 GeV/c^2 for selectrons with $M_{\tilde{e}_R} - M_\chi$ at least 3 GeV/c^2,
- 76 GeV/c^2 for mass degenerate sleptons if M_χ is smaller than 30 GeV/c^2, taking cascade decays into account.

The limit in the (m_0, M_2) plane under the assumption of scalar mass unification at the GUT scale is shown in Fig. 3. These results substantially extend the domains previously excluded at LEP.

Acknowledgements

It is a pleasure to congratulate our colleagues from the accelerator divisions for the successful operation of LEP above the W threshold. We would like to express our gratitude to the engineers and support people at our home institutes without whose dedicated help this work would not have been possible. Those of us from non–member states thank CERN for its hospitality and support.

References

[1] For a compilation of review articles, see: *Supersymmetry and Supergravity*, Ed. M. Jacob, North-Holland and World Scientific, 1986.

[2] OPAL Collaboration, Phys. Lett. **B 396** (1997) 301.

[3] DELPHI Collaboration, Phys. Lett. **B 387** (1996) 651;
L3 Collaboration, Phys. Lett. **B 377** (1996) 289;
OPAL Collaboration, Phys. Lett. **B 377** (1996) 273.

[4] ALEPH Collaboration, Phys. Lett. **B 373** (1996) 246.

[5] G. Farrar and P. Fayet, Phys. Lett. **B 76** (1978) 575.

[6] A. Bartl, H. Fraas and W. Majerotto, Z. Phys. **C 34** (1987) 411.

[7] ALEPH Collaboration, Nucl. Inst. Meth. **A 294** (1990) 121.

[8] ALEPH Collaboration, Nucl. Inst. Meth. **A 360** (1995) 481.

[9] H. Anlauf et al., Comp. Phys. Comm. **79** (1994) 466.

[10] S. Jadach and Z. Was, Comp. Phys. Comm. **36** (1985) 191.

[11] J.A.M. Vermaseren in *Proceedings of the IVth international Workshop on Gamma Gamma Interactions*, Eds. G. Cochard and P. Kessler, Springer Verlag, 1980.

[12] T. Sjöstrand, Comp. Phys. Comm. **82** (1994) 74;
T. Sjöstrand, CERN-TH 7112/93 (1993, revised August 1994).

[13] M. Skrzypek, S. Jadach, W. Placzek and Z. Was, Comp. Phys. Comm. **94** (1996) 216.

[14] S. Katsanevas and S. Melachroinos, in *Physics at LEP2*, Eds: G. Altarelli, T. Sjöstrand, F. Zwirner, CERN Report 96–01, Volume 2 (1996) 328.

[15] E. Barberio and Z. Was, Comp. Phys. Comm. **79** (1994) 291.

[16] S. Jadach, Z. Was, R. Decker and J.H. Kühn, Comp. Phys. Comm. **76** (1993) 361.

[17] ALEPH Collaboration, Phys. Lett. **B 384** (1996) 427

[18] R.A. Fisher, *The use of multiple measurements in taxonomic problems*, Annals of Eugenics **7** (1936) 179.

[19] The LEP Collaborations, *A Combination of Preliminary LEP Electroweak Measurements and Constraints on the Standard Model* CERN-PPE/96-183.

[20] ALEPH Collaboration, Phys. Rep. **216** (1992) 253.

[21] AMY Collaboration, Phys. Lett. **B 369** (1996) 86.

[22] K. Inoue, A. Kakuto, H. Komatsu and S. Takeshita, Prog. Theor. Phys. **68** (1982) 927; *ibid.* **71** (1984) 413;
H.P. Nilles, Phys. Rep. **110** (1984) 1;
H.E. Haber and G.L. Kane, Phys. Rep. **117** (1985) 75.